ELECTRON LINAC OPTIMIZATION FOR DRIVING BRIGHT GAMMA-RAY SOURCES BASED ON COMPTON BACK-SCATTERING

D. Alesini, A. Bacci, M. Bellaveglia, R. Boni, E. Chiadroni, G. Di Pirro, A. Esposito, M. Ferrario, A. Gallo, G. Gatti, A. Ghigo, A.R. Rossi, B. Spataro, P. Tomassini, C. Vaccarezza (INFN/LNF, Frascati), P. Antici , M. Migliorati, A. Mostacci, L. Palumbo (Univ. La Sapienza, Roma), F. Broggi, C. De Martinis, D. Giove, C. Maroli, V. Petrillo, L. Serafini (INFN/Milan and Univ. of Milan, Milano), A. Cianchi (Univ. of Tor Vergata, Roma)

Abstract

We study the optimal lay-out and RF frequency for a room temperature GeV-class Electron Linac aimed at producing electron beams suitable for Compton back-scattering based gamma-ray sources. These emerging technology of generating tunable, bright, mono-chromatic photon beams in the range 5-20 MeV for nuclear physics and nuclear engineering, relies on high quality electron beams, and J-class high rep-rate synchronized laser systems, to achieve the maximum spectral density of the gamma-ray beam (# photons/sec/eV). The best RF band among the most used in RF linacs (S, C, X) will be identified and discussed.

INTRODUCTION

We will first briefly delineate the concepts of Thomson back-scattering between two counter-propagating beams of electrons and optical photons, then considering the small Compton correction to the characteristics of the emitted back-scattered radiation, resume the analogy with ligth sources based on spontaneous emission of synchrotron radiation in undulators, and finally deriving the criteria for optimization of the colliding electron and laser beams. The best lay-out of the photo-Linac, in terms of its RF frequency band and operating conditions, will be derived applying the well known theory of high brightness beam production in photo-injectors[2], revisited here considering the requirements of a Compton gamma ray source. These are in fact somewhat different from those of FEL driving photo-Linacs, that aim at maximum beam brightness: we will see further on that our photo-Linac must aim at maximum 4-D transverse phase space density. A typical geometry of collision between the electron bunch and laser pulse to produce back-scattered X/γ photons is described in Fig.1. As for any collider, we can write the Luminosity of this Source as

$$L = \frac{N_L N_e}{4\pi\sigma_x^2} f \qquad [1]$$

where N_L is the number of optical photons carried by the laser pulse, N_e are the number of electrons in the electron bunch and σ_x is the rms electron spot size in the x-plane (round beams are assumed, $\sigma_x = \sigma_y$) - f is the rep rate of collisions, typically given by $f = f_{RF} n_{RF}$, the product between the RF rep rate f_{RF} and the number of bunches in each RF pulse n_{RF}. This equation holds in the case of well-matched beams at collision, in the focal region, in order to assure optimal space-time overlap.

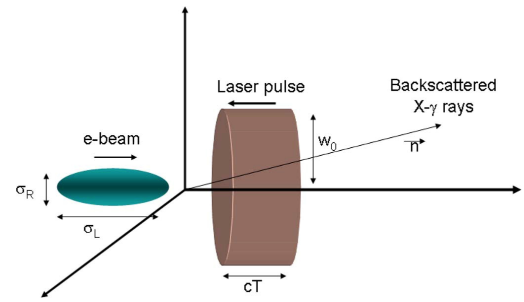

Figure 1: Thomson backscattering geometry. The electron beam of longitudinal and transverse sizes σ_L and σ_R, respectively, is moving at a relativistic speed from left to right, colliding with a photon beam of waist size w_0 and duration T, thus emitting scattered radiation mainly in the direction of motion of the electron beam.

Typical conditions that must hold are $w_0 \cong \sigma_x$ for transverse overlap, $cT < 2Z_R$ and $\sigma_z < \beta^* \equiv \gamma\sigma_x^2/\varepsilon_n$ to minimize the so called hour-glass effect (ε_n is the electron beam normalized rms emittance and γ its relativistic factor, $\gamma \equiv 1 + T_e/mc^2$). The total number N_γ of scattered photons is $N_\gamma = L\sigma_{TH}$, being $\sigma_{TH} = 0.67\cdot 10^{-28} m^2$ the Thomson cross-section. In more practical notations

$$N_\gamma = 2.1\cdot 10^8 \frac{U_L[J]Q[pC]}{h\nu[eV]\sigma_x^2[\mu m]} f \qquad [2]$$

where U_L and Q are the laser pulse energy and the electron bunch charge. For a typical set of parameters of interest for a gamma ray Compton Source, we have $U_L = 1\ J$, $Q = 250\ pC$, $h\nu = 2.4\ eV$, so that a focal spot size of $\sigma_x = 30\ \mu m$ gives a number of photons/sec $N_\gamma = 2.4\cdot 10^{11}$ ($f = 10^4$) emitted over all the solid angle and frequency spectrum, with an associated source luminosity $L = 3.7\cdot 10^{35} cm^{-2} sec^{-1}$.

The frequency ν_γ of radiation emitted within a small angle of scattering and electron incidence θ around the propagation axis of the electron beam is given by

$$\nu_\gamma = \nu_L \frac{4\gamma^2}{1+\gamma^2\theta^2 + a_0^2/2}(1-\Delta) \qquad [4]$$

where ν_L is the laser optical frequency, a_0 the laser parameter and the dimensionless parameter $\Delta = \frac{4\gamma h\nu_L / mc^2}{1+2\gamma h\nu_L / mc^2}$ represents the red-shift due to electron recoil (*i.e.* inelastic Compton scattering versus elastic Thomson scattering). In a practical example of interest here, an electron at 720 MeV of kinetic energy colliding head-on ($\theta = 0$) with a 1 J, 500 nm laser pulse (2.4 eV), focused down to 15 μm ($a_0 = 0.07$) would scatter back along its propagation direction a 19 MeV gamma photon if elastic Thomson scattering is considered. When the Compton recoil is taken into account ($\Delta = 0.027$), the effective gamma photon energy is found to be 18.5 MeV.

At this point we are interested to know what is the number of photons emitted in a small forward cone and which is the associated bandwidth, including the effects of bandwidth enhancement due to the rms spreads of the electron beam in its transverse and longitudinal phase spaces. Looking at the dependence of the scattered photon frequency on the electron energy, angle and laser parameter as in eq.4, we can easily deduce that the bandwith is given by 5 contributions:

$$\frac{\Delta\nu_\gamma}{\nu_\gamma} \cong 2\frac{\Delta\gamma}{\gamma} + (\gamma\vartheta_M)^2 + 2\left(\frac{\varepsilon_n}{\sigma_x}\right)^2 + \frac{a_0^2}{1+a_0^2} + \frac{\Delta\nu_L}{\nu_L} \quad [5]$$

being the first due to the electron beam energy spread $\Delta\gamma/\gamma$, the second to the observation angle ϑ_M (or the collecting angle of our detector), the third due to inherent crossing angle $\gamma\sigma_{x'} = \varepsilon_n/\sigma_x = \sigma_{px}$ of the electron trajectory in the focal region (where collision takes place) averaged over the electron beam phase space (cfr. emittance), the fourth one to the laser field variation along the pulse (going in time from 0 to its maximum value of a_0) and the fifth one due to the laser bandwidth $\Delta\nu_L$. It is clear that the minimum bandwidth is achieved when the collecting angle is set equal to (and we define the quantity Ψ accordingly)

$$\Psi_{\min}^2 \equiv (\gamma\vartheta_M)_{\min}^2 \cong 2\frac{\Delta\gamma}{\gamma} + 2\left(\frac{\varepsilon_n}{\sigma_x}\right)^2 + \frac{a_0^2}{1+a_0^2} + \frac{\Delta\nu_L}{\nu_L} \quad [6]$$

Decreasing the collecting angle below this value would not decrease the bandwidth of the radiation but only the photon flux. Hence, eq.6 sets the collecting angle corresponding to maximum spectral density. In reference 1 the number of photons emitted within a small angle $\Psi \equiv \gamma\vartheta$, together with detailed calculations of the associated bandwidth, are derived, giving:

$$\frac{\Delta\nu_\gamma}{\nu_\gamma} = \frac{\Psi^2}{1+\Psi^2/2} \; ; \; \Psi > \Psi_{\min} \quad [7a]$$

$$N_{\gamma bw} = 4.6 \cdot 10^8 \frac{U_L[J]Q[pC]f}{h\nu[eV]\sigma_x^2[\mu m]} \frac{\Psi^2}{(1+\Psi^2)^2} \quad [7b]$$

which gives, for the same set of parameters above, *i.e.* $U_L = 1\ J$, $Q = 250\ pC$, $\sigma_x = 30\ \mu m$, $\varepsilon_n = 0.29\ \mu m$, $a_0 = 0.03$, $\Delta\gamma/\gamma = 0.095\%$, $\Psi = 0.055$, $f = 10^4$, $\frac{\Delta\nu_\gamma}{\nu_\gamma} = 0.003$ and $N_{\gamma bw} = 1.6 \cdot 10^9\ ph/sec$. The angle of emission is given by $\vartheta = \Psi/\gamma$. The best accelerator for such a source is the one attaining the maximum value for the parameter $\frac{Q}{\sigma_x^2\left[\Delta\gamma/\gamma + (\varepsilon_n/\sigma_x)^2\right]}$ which scales like the spectral density (photons/sec/eV) of the emitted radiation, as far as the electron beam contribution is concerned. Since a photo-Linac delivering a high brightness electron beam handles in a somewhat uncoupled way the longitudinal and transverse phase spaces (in particular when no bunch compression is needed as in present case), we can assume that the emittance si minimized for a given charge independently on the beam energy spread, so the relevant parameter, sort of a quality factor η, for the optimization of the lay-out and operating frequency of a photo-Linac, will be $\eta \equiv Q/\varepsilon_n^2$, which actually represents the density in the 4-D transverse phase space. Worth to note that maximum spectral density of the gamma ray beam is reached for the maximum phase space density of the electron beam.

The optimal conditions to achieve maximum phase space density in a photo-Linac are set by the invariant envelope theory (see ref.2), describing the electron beam as a single component relativistic plasma propagating paraxially from the photo-cathode placed inside the RF gun up to the Linac exit, under the effect of its own space charge field, the RF focusing of accelerating sections and the acceleration damping due to the strong field gradient applied. Under the conditions of invariant envelope and optimum phasing of space charge oscillations (see ref.3) the final emittance is almost compensated down to the thermal emittance value given by cathode emission. So we expect an emittance scaling like $\varepsilon_n \propto \sigma_{cat} \propto Q^{1/2}$, which is actually found approximately in simulations (see below a scaling found as $\varepsilon_n \propto Q^{0.58}$). This means that the spectral density factor $\eta \propto Q/\varepsilon_n^2 \propto 1$ would almost be independent on bunch charge: we will see actually that simulations predict a slight dependence that favours small bunch charges, below 200 pC for the RF frequency bands taken into consideration here (S-band, C-band and X-band).

In the numerical analysis we considered two different lay-outs: for S-band and C-band we considered a standard 1+1/2 cell RF gun injecting into a sequence of travelling wave accelerating section, with matching onto the Ferrario working point, taking into account the thermal emittance at the cathode (0.6 μm per mm of photocathode spot size σ_{cat}). The maximum gradients adopted in simulations for the S-band (2.856 GHz) and C-band (5.712 GHz) sections were 25 and 40 MV/m, respectively. For the X-band (11.424 GHz) photo-Linac we adopted a 5+1/2 cell RF gun, which was already tested and operated up to 200 MV/m, properly matched to X-band accelerating structures with gradient of 60 MV/m.

We performed an extensive campaign of numerical based optimizations, carried out with ASTRA and GIOTTO: a standard code for beam dynamics studies of high brightness electron beams (ref.5), typically used in the FEL community, and a genetic algorithm based code to perform optimizations of multi-dimensional highly non-linear problems (ref.4). Optimization is performed by iterative runs of ASTRA over the many free parameters of the problem, until best result is found in terms of minimum emittance ε_n at the exit of the Linac (with typical beam energies around 600 MeV). The genetic algorithm search is carried out over the values of the cathode launching phase, the magnetic focusing solenoid field amplitude, the laser spot size at the cathode, its length (we assumed uniform laser intensity distribution in time and transverse plane), the phases and gradients of following accelerating sections. Each values reported in the following Tables is the result of the genetic algorithm optimization carried out over hundreds of single runs spanning the operating range of dynamical free parameters. We considered the state of the art peak field on the cathode for the S-band case (120 MV/m), three levels for C-band (170, 200 and 240) and the reference one for X-band (200 MV/m).

Table 1: S-band at 120 MV/m

Q [pC]	ϵ_n[μm]	Q/ϵ_n^2 [pC/μm^2]	B_n[A/m^2] (I [A])
1000	0.76	1731	2.1e14 (56)
575	0.55	1901	2.3e14 (35)
500	0.537	1734	2.6e14 (38)
250	0.361	1918	2.7e14 (17)

Table 2: C-band at 200 MV/m

Q [pC]	ϵ_n[μm]	Q/ϵ_n^2 [pC/μm^2]	B_n[A/m^2] (I [A])
500	0.433	2667	5.2e14 (49)
250	**0.29**	**2972**	**6.7e14 (28)**
100	0.18	3086	9.7e14 (16)
50	0.126	3149	1.1e15 (8)

Table 3: X-band at 200 MV/m

Q [pC]	ϵ_n[μm]	Q/ϵ_n^2 [pC/μm^2]	B_n[A/m^2] (I [A])
500	0.578	1497	4.8e14 (81)
250	0.317	2488	9.2e14 (46)
100	0.19	2770	1.4e15 (25)
20	0.085	2768	2.4e15 (8.6)

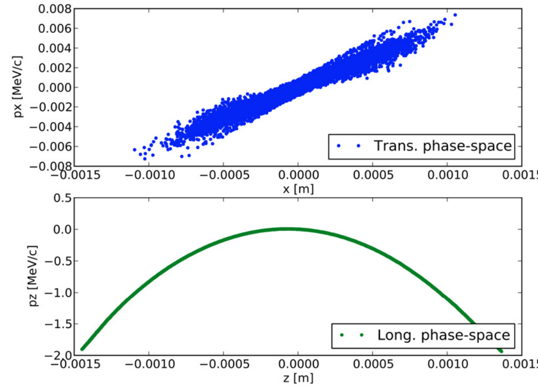

Figure 2: Transverse and longitudinal phase space distributions for best case selected, 250 pC at C-band, 200 MV/m (see Table 2)

We should remark that this analysis was performed looking for maximum phase space density η of the beam at the end of the photo-Linac, not for beam brightness (which is the peak beam phase space density normalized to its bunch length, $B_n \propto \frac{Q}{\sigma_z \varepsilon_n^2}$), as usually done for Linacs driving FELs. In order to have an easy to use criteria, and since this comprehensive analysis of beam dynamics in photo-Linacs was never performed since, we list some useful scaling laws for the emittance as a function of bunch charge for the 5 cases under study.

$$\varepsilon_n^{Sband-120} = 0.0138 \cdot Q^{0.58}$$
$$\varepsilon_n^{Cband-170} = 0.01385 \cdot Q^{0.58}$$
$$\varepsilon_n^{Cband-200} = 0.01189 \cdot Q^{0.58}$$
$$\varepsilon_n^{Cband-240} = 0.01162 \cdot Q^{0.58}$$
$$\varepsilon_n^{Xband-200} = 0.01857 \cdot Q^{0.5} + 1.035 \cdot 10^{-8} Q^{8/3}$$

nicely confirming that emittance compensation was performed almost ideally down to the thermal emittance minimum level, as shown by the transverse phase space plotted in Fig.2, which does not exhibit almost any distortions but nearly only thermal emittance contributions.

Simulations of the Compton gamma ray Source, by colliding the selected electron beam with a 1 J laser, under optimal focusing conditions, predict $N_\gamma = 1.5 \cdot 10^9$ photons/sec at *E=11* MeV, within a bandwith $\Delta\nu_\gamma/\nu_\gamma = 0.25\%$, with $f = 10^4$, ($f_{RF} = 100$ $n_{RF} = 100$) equivalent to a spectral density 5.3·10^4 photons/sec/eV.

REFERENCES

[1] P. Tomassini et al., Appl. Phys. B 80, 419–436 (2005)
[2] L. Serafini et al., Physical Review E 55, 6 (1997)
[3] M. Ferrario et al., Phys. Rev. Lett. 104, 054801 (2010)
[4] A. Bacci et al., NIM A-608, 93 (2009)
[5] K. Flottmann, http://www.desy.de/~mpyflo/